Theory of high-field-domain structures in superlattices

D. Miller and B. Laikhtman
Racah Institute of Physics, Hebrew University, Jerusalem 91904, Israel
(Received 17 December 1993; revised manuscript received 31 May 1994)

A number of experimental works provide evidence for the existence of high-field domains in superlattices when the applied voltage exceeds some critical value. A theoretical description of the structure of such a domain is developed. We confine ourselves to the case of narrow-band superlattices, where electrons are strongly localized in the wells. We find that the minimum length of the high-field domain can be larger than one superlattice period. The maximum current in the oscillating part of the I-V characteristic can be significantly smaller than the value of the current at the voltage where the first instability comes about. The oscillation period can be considerably smaller than the value corresponding to the energy separation between the first and second level in a well. For the case of the domain formation at some distance from the anode, we study the field distribution in the low-field region downstream of the domain.

I. INTRODUCTION

During the past 20 years a number of interesting experimental works have been performed in order to investigate transport properties of superlattices in growth direction.[1–12] Under a weak applied bias the superlattice looks like a homogeneous medium and exhibits Ohm's law. Near some critical field $F_{\rm th}$ an instability appears and destroys the homogeneous state. As a result of the instability the superlattice breaks down into three regions: the low-field region with transport in the first miniband, the high-field domain, and the low-field region where electrons are injected into the second miniband from the high-field domain and then relax down to the first miniband; see Fig. 1. An electron can move 1000 Å in the second miniband before it drops down[13–15] because the intersubband relaxation rate is relatively small. A further increase of the applied bias leads to an expansion of the high-field region and the current exhibits an oscillatory behavior. The period of this oscillation can be associated with the intersubband space, but generally it is smaller.[4,2] Under higher biases upper minibands become involved in the transport process.

A phenomenological model that described a superlattice by an equivalent electric circuit was suggested by one of the authors.[16] In this model each barrier was replaced by a nonlinear resistor parallel to the capacitor. The model explained current oscillations and the hysteresis usually observed in the experiment. Prengel, Wacker, and Schöll[17] considered a model for a realistic superlattice which included electron tunneling between different levels in the adjacent wells and relaxation processes inside one well. They obtained multistability of the current-voltage characteristic and various hysteretic transitions which arose upon sweeping the applied voltage and which they associated with changes in the domain size.

The purpose of the present work is not to simulate the I-V characteristics in a specific superlattice but to understand the general structure of the high-field domain. A diffusion current induced by a charge accumulation at the domain boundary appears to be very important. We calculate the field and the carrier distribution in the steady state and get the main features of the current-voltage characteristic of the superlattice in some interval of the applied bias. The size and the position of the domain are also discussed.

The physical processes characterizing transport in a superlattice are described briefly in the next section. In Sec. III we derive the equation for the hopping current between two levels in the different wells. In Secs. IV, V, and VI we calculate the field distribution in regions I, II, and III, correspondingly. We discuss the results and make some comparisons with available experimental data in Sec. VII.

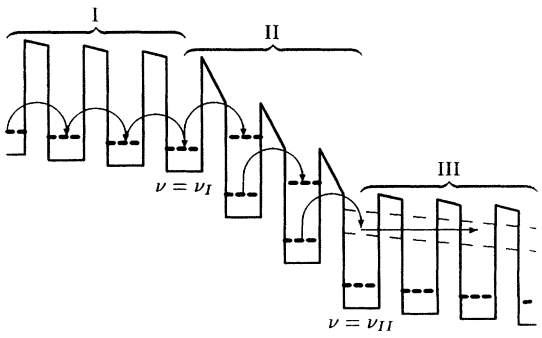

FIG. 1. Regions of different conductivity in the superlattice. I and III are low-field domains and II is a high-field domain. Dashed lines show the levels position. Levels are broadened due to scattering. The second levels in region III form a miniband and long dashed lines show its edges. Arrows show the hopping of electrons between the levels. In region III most of the electrons move in the second miniband. If the domain is formed near the anode, region III does not exist.

II. PHYSICAL PICTURE

Let us see what happens when the bias applied to the superlattice increases and goes beyond the instability threshold. If as a result of the instability development a narrow high-field domain is spontaneously generated,[1] then the field in the low-field regions is reduced by F_H/N, where F_H is the field in the high-field region and N is the number of the superlattice periods. The current in the low-field region is $j \approx 2j_0 F F_{\rm th}/(F^2 + F_{\rm th}^2)$, where $F_{\rm th}$ is the threshold field and j_0 is the current just before the instability point.[18] So the generation of the narrow domain results in the reduction of the current by $\delta j \approx j_0 (F_H/F_{\rm th}N)^2$. Usually F_H is only 10 or 15 times larger than $F_{\rm th}$, but the number of periods can range from 50 to 100 and therefore the reduction of the current is small $\delta j \ll j$.

The formation of the high-field domain is accompanied by the accumulation of electrons in the well just upstream of the domain and with the depletion of electrons in the well just downstream of the domain. The accumulation of electrons in one well gives rise to a diffusion current upstream of this well in the direction opposite the total current. Since the total current is the same across all of the barriers, the diffusion current across one barrier has to be compensated for with the conduction part of the current. It may occur that this compensation is impossible because the electric current is too close to its maximum value j_0, that is, for a such a value of the total current a steady state does not exist. A steady state can come about only for a domain extended enough when the total current is not too close to its maximum value j_0. Therefore there exists a minimum length of the high-field domain and the upper limit of the total current in a steady state j^*.

Generally, after the formation of the high-field domain with an increase of the applied bias, the total current drops below j^*. A further increase of the bias leads to the growth of the current and when it reaches j^* the high-field domain expands by one period and the current drops again.

The change of the potential drop across the high-field domain when it expands by one period is usually associated with the energy space $\mathcal{E}$ between the first and second levels in a well.[1,3–5,8–10] It is assumed that in the high-field domain the first level in one well is in resonance with the second level in the neighbor well. The number of electrons in the first $n^{(1)}$ and second $n^{(2)}$ levels can be found from the simple balance equation

$$\frac{n^{(1)} - n^{(2)}}{\tau_t} = \frac{n^{(2)} - n^{(1)} e^{-\mathcal{E}/T}}{\tau_{21}} , \qquad (1)$$

where $n^{(1)} + n^{(2)} = \bar{n}$ is the total concentration. Here $\tau_t = \hbar\Gamma/\Lambda_{12}^2$ is the transition time between adjacent wells,[19] Γ is the width of the level, Λ_{12} is the overlap between the wave functions of the first level in one well and the second level in the adjacent well, and τ_{21} is the relaxation time from the second level to the first one in the same well. If $\tau_t \ll \tau_{21}$, then the current is $e\bar{n}[1 - \exp(-\mathcal{E}/T)]/2\tau_{21}$. This current has to be smaller than j^*, which does not always take place. If $\tau_t \gg \tau_{21}$ the current is $e\bar{n}\tanh(\mathcal{E}/T)/\tau_t$. However, this quantity is even larger than $j_0 = e\bar{n}\Lambda_{11}^2/\max(E_F, T)$, where Λ_{11} is the overlap between the wave functions of the first levels in adjacent wells; see Ref. 18.

We see that under resonance conditions the current in the high-field domain sometimes appears to be larger than the maximum possible current in region I and such a regime cannot exist. Due to the limitation of the current in region I, resonance in region II is not reached. The current in this region is smaller than its resonance value for two reasons. The tunneling probability is reduced because of a lack of resonance and not all electrons in the second level in one well have enough energy to move to the first level in the neighbor well.

If the resonance between the first and the second level in adjacent wells does not exist, the expansion of the high-field domain by one period requires a voltage increase smaller than that corresponding to $\mathcal{E}$. This is the explanation of a small period of the current oscillations sometimes observed in experiments.[2–4,8]

The well at the boundary between regions II and III is depleted. The reduction of the electron concentration in this well corresponds to field discontinuity between the high-field domain and region III. If the necessary reduction is larger than the average electron concentration in a well, then the domain is located near the anode, where a depletion layer is formed.[10]

In doped superlattices electrons come from the high-field domain to the second miniband in region III and relax there down to the first miniband. The relaxation length depends on the relation between the mobilities in the first and second minibands and an intersubband relaxation time. The redistributing of electrons between two minibands can result in a field inhomogeneity in region III.

III. ELECTRIC CURRENT BETWEEN ADJACENT WELLS

In this work we consider the case of elastic scattering so strong that an electron is scattered in a well before tunneling to the next well, at least in the first miniband. So for the calculation of the current we need the transition probabilities between adjacent wells. Since the widths of levels are typically much smaller than the energy separations between them, only the tunneling between those levels that are close to resonance is important.

The general form of the transition probability between such levels is

$$w \propto \frac{\Lambda^2}{\hbar} \frac{\Gamma}{\Gamma^2 + \Delta^2} , \qquad (2)$$

where Δ is the energy separation between levels. In the low-field region this equation describes the transition between lowest levels and it is justified for $\Lambda_{11} \ll \Gamma$; see Ref. 18. For the transition from the first level to the second level in the adjacent well such an equation was derived by Kazarinov and Suris.[19] In this case Eq. (2) is justified for an arbitrary relation between Λ and Γ.

The overlap integral Λ and the level width due to elastic scattering Γ are different for different pairs of levels. The overlap integral increases with the level number because the wave function penetration length under the barrier increases with the energy. The parameter Γ in Eq. (2) is different for the transition from the first level to the first level and for the transition from the first level to the second level because in the latter case the presence of the first level gives more possibilities for momentum relaxation.

In a part of region III electrons can travel in the second subband, which can be wide. Therefore in this region instead of Eq. (2) we use Ohm's law.

The transition probability Eq. (2) gives the following expression for the electric current from the ith level in the νth well to the i'th level in the $\nu+1$th well:

$$j_{ii'} = \frac{e}{\hbar}\int \frac{2d\mathbf{p}}{(2\pi\hbar)^2}\frac{2\Gamma\Lambda_{ii'}^2}{\Gamma^2+\Delta_{\nu,ii'}^2}\left[\rho(E_p)-\rho'(E_p+\Delta_{\nu,ii'})\right] \tag{3a}$$

when the level in the νth well is higher $\Delta_{\nu,ii'}>0$ and

$$j_{ii'} = \frac{e}{\hbar}\int \frac{2d\mathbf{p}}{(2\pi\hbar)^2}\frac{2\Gamma\Lambda_{ii'}^2}{\Gamma^2+\Delta_{\nu,ii'}^2}\left[\rho(E_p-\Delta_{\nu,ii'})-\rho'(E_p)\right] \tag{3b}$$

when the level in the νth well is lower $\Delta_{\nu,ii'}<0$. In these equations $\Lambda_{ii'}$ is the overlap integral between electron wave functions of the levels i and i' in the νth and $(\nu+1)$th wells correspondingly. The energy space between these two levels is denoted by $\Delta_{\nu,ii'}$. The diagonal elements of the electron density matrix related to these two levels ρ and ρ' can be considered as a function of the energy $E_p=\mathbf{p}^2/2m$, where m is effective mass of electrons, since the in-plane motion of electrons is isotropic and this density matrix element is independent on the direction of $\mathbf{p}$. Usually Γ is a smooth function of the energy and we assume it to be a constant.

We see from Eq. (3) that the value of the current depends on the shape of the electron distribution function. Equation (3) is simplified in three cases. The first is the case of a weak electron heating when the electron distribution function is close to the equilibrium one.

In the second case the electron gas is degenerate and Δ is smaller than the Fermi energy. Then the difference of the distribution function in the integrands of Eq. (3) is proportional to Δ and the tail of the distribution function above the Fermi energy does not play any role.

In the third case the electron gas is heated significantly so that the electron-electron scattering is very effective and leads to a fast relaxation of the electron distribution function to the Fermi function with an effective temperature T and a chemical potential $\zeta_\nu^{(i)}$, where ν is the index of the well and i is the index of the level. We should note, however, that even a strong deviation of the electron distribution from the Fermi function does not change qualitative results of the present work.

Under these assumptions the integration in Eq. (3) results in

$$j_{ii'} = \frac{2e\Lambda_{ii'}^2}{\hbar}\frac{\Gamma}{\Gamma^2+\Delta_{\nu,ii'}^2}\left[n_\nu^{(i)}-n(\zeta_{\nu+1}^{(i')}-\Delta_{\nu,ii'})\right] \tag{4a}$$

when the level in the νth well is higher and

$$j_{ii'} = \frac{2e\Lambda_{ii'}^2}{\hbar}\frac{\Gamma}{\Gamma^2+\Delta_{\nu,ii'}^2}\left[n(\zeta_\nu^{(i)}+\Delta_{\nu,ii'})-n_{\nu+1}^{(i')}\right] \tag{4b}$$

when the level in the νth well is lower. In these two equations

$$n_\nu^{(i)} = n(\zeta_\nu^{(i)}) \equiv g_0 T\ln(e^{\zeta_\nu^{(i)}/T}+1) \tag{5}$$

is the concentration of electrons in the νth well at the ith level and $g_0=m/\pi\hbar^2$. We will omit the subscripts of Δ when it does not lead to confusion. The barrier for the second level is lower than for the first level, so one can expect that $\Lambda_{11}<\Lambda_{12}<\Lambda_{22}$.

The difference in the square brackets in Eq. (4) can be simplified

$$n_\nu^{(i)}-n(\zeta_{\nu+1}^{(i')}-\Delta_{\nu,ii'}) = n_\nu^{(i)}-n_{\nu+1}^{(i')}+\Delta_{\nu,ii'}\left(\frac{\partial n}{\partial\zeta}\right)_{\zeta_{\nu+1}^{(i')}} \tag{6}$$

in either of two cases $\zeta-\Delta\gg T$ or $\zeta\lesssim T$, $\Delta\ll T$.

In the case when expansion Eq. (6) is used one can distinguish between the diffusion current and the conduction current. The former is proportional to the concentration difference and the later is proportional to Δ. Note that

$$\left(\frac{\partial n}{\partial\zeta}\right)_{\zeta_{\nu+1}^{(i')}} \equiv g = g_0\left(1-e^{-n_{\nu+1}^{(i')}/g_0T}\right) \tag{7}$$

is not a constant, but depends on the electron concentration, which can be different for different levels.

IV. LOW-FIELD REGION UPSTREAM OF THE DOMAIN

We assume that in the low-field region upstream of the domain there are electrons in the first miniband only. Motion of electrons in the narrow miniband $\Lambda\ll\Gamma$ can be described in terms of hopping between adjacent wells.[18] So, a current via each barrier can be found from Eq. (4a), where $i=i'=1$ and these indices will be omitted throughout this section.

The electric field in this low-field region is inhomogeneous only near the boundary with the high-field domain. The field distribution near this boundary can be calculated from Poisson equation together with the condition that the current is the same through all barriers in this region. One can see from Eq. (4a) that the current through a barrier is a nonlinear function of the electron concentration near this barrier, and of the field in this barrier, $\Delta/(ed)$. For simplicity we consider only the degenerate electron gas. In this case $\partial n/\partial\zeta$ in Eq. (6) is a constant;

it is equal to g_0; see Eq. (7). This restriction is not very strong since additional electrons come to this region from region III if it exists or from the anode contact. Therefore the electron gas in region I near the boundary of the high-field domain is typically degenerate.

In this case the condition that allows us to use the expansion Eq. (6) is $\Delta_\nu < n_{\nu+1}/g_0$. Since the current in the superlattice with the high-field domain is smaller than j_0, the potential drop per period far from the domain boundary in region I is small, i.e., $\Delta < \Gamma$. On the other hand, the theory is limited by the condition $\Gamma \lesssim E_F$ and we see that far from the domain $\Delta < E_F$. The field in the barriers increases with approaching the high-field domain boundary; however, the electron concentration also increases and the necessary condition is usually fulfilled. It makes sense to note that the necessary condition contains the concentration upstream of the barrier where it is larger than that downstream.

We introduce here two quantities which can be measured in practice. The first of them is the linear conductivity in the low subband σ. One can find from Eqs. (4)–(7) that $\sigma = 2e^2 g d \Lambda_{11}^2/\hbar\Gamma$; see also Ref. 18. The second one is the critical field $F_{\rm th}$. This field corresponds to the instability of the homogeneous steady state. In Ref. 18 it was shown that $F_{\rm th} \approx \Gamma/ed$. The substitution of this quantity into Eq. (4a) gives, for $\nu < \nu_I$, where ν_I is the number of the well between regions I and II (see Fig. 1),

$$j = \frac{\sigma}{d}\,\frac{\phi_\nu - \phi_{\nu+1} + (n_\nu - n_{\nu+1})/eg}{1 + [(\phi_\nu - \phi_{\nu+1})/F_{\rm th} d]^2} \,. \tag{8a}$$

Here ϕ_ν is the diagonal matrix element of the electric potential in the νth well. The contribution to the current proportional to the concentration difference on the right-hand side of Eq. (8a) can be considered as a diffusion current. In region I the electron concentration grows in the vicinity of the high-field domain and therefore the direction of the diffusion current is opposite the direction of the total current. In terms of these potentials $\Delta_{\nu,ii'} = e\phi_\nu - e\phi_{\nu+1}$.

The given definition of the potentials allows us to avoid the consideration of the well polarization. This effect is taken into account in Ref. 18, where the integrated Poisson equation was derived. It provides the necessary connection between potentials ϕ_ν and concentrations n_ν

$$\Delta_\nu[\phi] + \frac{e}{C_{\rm eff}}\Delta_\nu[n] = -\frac{4\pi e d}{\bar\epsilon}(n_\nu - \bar n) \,. \tag{8b}$$

Here $C_{\rm eff}$ and $\bar\epsilon$ are constants, which can be calculated for a given superlattice $\Delta_\nu[f] \equiv f(\nu+1) + f(\nu-1) - 2f(\nu)$ and $\bar n$ is the average electron concentration. The second term on the left-hand side of Eq. (8b) describes the capacitance of one well.[18]

The system Eqs. (8) has two boundary conditions. First, when the ν goes to $-\infty$ the difference $\phi_\nu - \phi_{\nu+1}$ goes to $F_\infty d$. Second, Eq. (8b) for $\nu = \nu_{\rm I}$ contains the difference $\phi_{\nu_{\rm I}} - \phi_{\nu_{\rm I}+1}$, which is defined by the field in the high-field region F_H and therefore it is about $F_H d$. Far from the boundary with region II Eq. (8a) becomes

$$j = \frac{\sigma F_\infty}{1 + (F_\infty/F_{\rm th})^2} \,. \tag{9a}$$

It shows that the current in region I is limited from above and reaches the maximum at $F_\infty = F_{\rm th}$

$$j < j_0 = \frac{1}{2}\sigma F_{\rm th} \,. \tag{9b}$$

It is convenient to introduce a dimensionless field f_ν and displacement h_ν as

$$f_\nu = \frac{2[(\phi_\nu - \phi_{\nu+1})/d - F_\infty]F_\infty}{3(F_{\rm th}^2 - F_\infty^2)} \,, \tag{10a}$$

$$h_\nu - h_{\nu-1} = \frac{8\pi e F_\infty/\bar\epsilon}{3(F_{\rm th}^2 - F_\infty^2)}(n_\nu - \bar n) \,, \tag{10b}$$

where $\nu \le \nu_{\rm I}$. Equations (8) take the form

$$f_\nu - \lambda_1^{-2}\Delta_\nu[h] - \tfrac{3}{2}(f_\nu)^2 = 0 \,, \tag{11a}$$

$$h_\nu + \lambda_2^{-2}\Delta_\nu[h] - f_\nu = 0 \,, \tag{11b}$$

where

$$\lambda_1^2 = \frac{4\pi e^2 g d}{\bar\epsilon}\,\frac{F_{\rm th}^2 - F_\infty^2}{F_{\rm th}^2 + F_\infty^2} \,, \tag{12a}$$

$$\lambda_2^2 = \frac{4\pi d C_{\rm eff}}{\bar\epsilon} \,. \tag{12b}$$

The boundary conditions for Eqs. (11) are

$$\lim_{\nu\to-\infty} f_\nu = 0 \,, \tag{13a}$$

$$f_{\nu_{\rm I}} = \frac{2(F_H - F_\infty)F_\infty}{3(F_{\rm th}^2 - F_\infty^2)} \,. \tag{13b}$$

The coefficient λ_2 depends only on superlattice parameters. From the definitions of the $\bar\epsilon$ and $C_{\rm eff}$ in Ref. 18 one can easily get that $\lambda_2 > 2$. The parameter λ_1 depends on F_∞ and therefore on the current through the superlattice $\lambda_1^2 \propto \sqrt{1 - j^2/j_0^2}$; see Eqs. (9) and (12a). Therefore λ_1 goes to zero when the current approaches its maximum value.

The analytic solution to nonlinear difference equations Eqs. (11) can be obtained in some limit cases, but we consider here only one important example. Later we give the numerical solution in the general case.

For $\lambda_1 \ll 1, \lambda_2$, the variation of f_ν and h_ν from well to well is small. Hence the second difference $\Delta_\nu[\,]$ can be replaced with the second derivative $d^2/d\nu^2$ and it can be neglected in Eq. (11b). The resulting differential equation has the solution

$$h_\nu = f_\nu = \frac{1}{\cosh^2(\lambda_1\nu/2 + \text{const})} \,. \tag{14}$$

The constant in Eq. (14) can be found from the boundary condition Eq. (13b). The important property of this solution is that it is limited from above. Such a limitation is not connected with a small value of λ_1, but it is a general property of Eq. (11). This limitation ultimately results from the limitation of the current in the

first miniband; see, e.g., Eq. (9a). In general, the upper limit of the solution to Eq. (11), which satisfies boundary condition Eq. (13a), depends on λ_1 and λ_2:

$$f_{\nu_I} < \Upsilon(\lambda_1, \lambda_2) \ . \tag{15}$$

Equations (11) can be reduced to the recurrent relation

$$f_{\nu-1} = \mathcal{G}(f_\nu) \ , \tag{16}$$

where the function $\mathcal{G}(x)$ depends on the parameters λ_1 and λ_2 and does not depend on ν. This function has to satisfy the boundary condition Eq. (13a), i.e., $\mathcal{G}(x)$ vanishes when x goes to zero. For $x \ll 1$ the function $\mathcal{G}(x)$ can be calculated explicitly.

Typical plots for $\mathcal{G}(x)$ are shown in Fig. 2. One can get the sequence of values of f_ν by iteration of the function $\mathcal{G}(x)$. For example, $f_{\nu_I-2} = \mathcal{G}(\mathcal{G}(f_{\nu_I}))$; f_{ν_I} is given by Eq. (13b). These iterations are shown in Fig. 2 by dashed lines. One can see that

$$\Upsilon = \max\left[\mathcal{G}^{-1}(x)\right] \ , \tag{17}$$

where $\mathcal{G}^{-1}(x)$ is the function inverse to $\mathcal{G}(x)$, $\mathcal{G}\left(\mathcal{G}^{-1}(x)\right) = x$. The position of this maximum is also marked in Fig. 2 by a square. In Fig. 3 this maximum Υ is plotted as a function of λ_1^2 for different values of λ_2^2.

A calculation[18] shows that $\lambda_2^2 \geq 4(d_B\epsilon_{\text{eff}}/d_W\epsilon + 1)$, where d_B and d_W are the widths of the barrier and the well, respectively, ϵ is dielectric constant in the barrier, and ϵ_{eff} is the effective dielectric constant in the well.

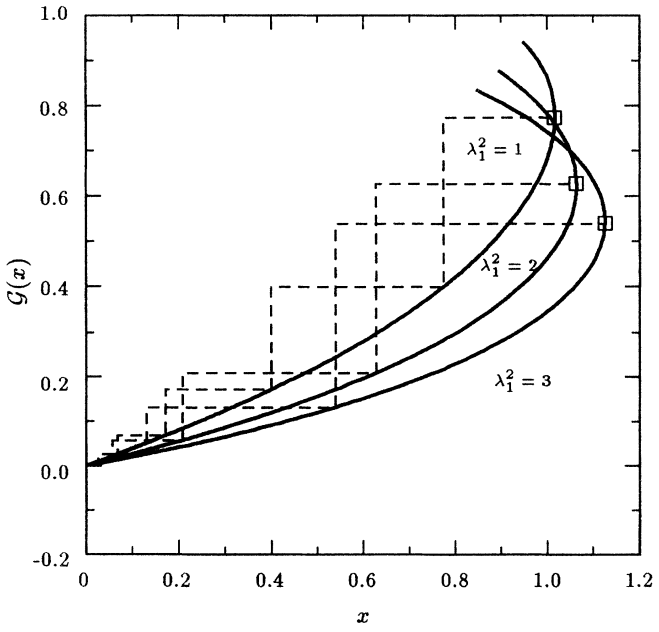

FIG. 2. $\mathcal{G}(x)$ for different values of λ_1^2 and $\lambda_2^2 = 20$. The quantities f_ν, which are proportional to the electric field in the barrier ν, can be obtained by iteration of the function $\mathcal{G}(x)$ and the dashed lines show the example of such an iteration. The iteration starts from the value of f that corresponds to the field in the high-field domain. Squares show the maximum value of that f.

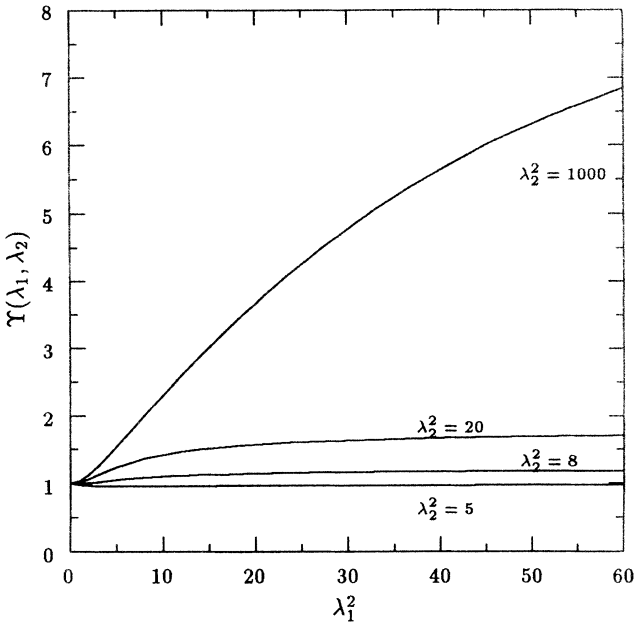

FIG. 3. Υ as a function of λ_1^2 is plotted for different values of λ_2^2.

Although ϵ_{eff} is proportional to a number of electrons in the well, usually $\epsilon_{\text{eff}} \sim \epsilon$ and $d_B \sim d_W$. Thus a typical value of λ_2^2 is 8–10. It becomes large only in the limit of extremely narrow wells or very highly doped wells. The other parameter λ_1^2 can be estimated by means of Eq. (12a). It gives $\lambda_1^2 < e^2 g_0 d = d/24$ Å. Even if the superlattice period is 500 Å, $\lambda_1^2 < 20$. We plot Υ for λ_1^2 that ranges from 0 to 60; see Fig. 3. The estimation for typical values of λ_1^2 and λ_2^2 shows that usually $\Upsilon \approx 1$.

The condition Eq. (15) can be rewritten in terms of the current j by making use of Eqs. (13b) and (9)

$$j < j^* \ , \tag{18}$$

where j^* can be found from

$$\frac{j^*}{j_0 + (3\Upsilon - 1)\sqrt{j_0^2 - (j^*)^2}} = \frac{F_{\text{th}}}{F_H} \ . \tag{19}$$

The quantity j^* is the upper limit of the current in the superlattice with the high-field domain. The current through the superlattice is also limited by Eq. (9b), but $j^* < j_0$ and therefore Eq. (18) is a more strong restriction. This restriction comes from the properties of the boundary between regions I and II. Indeed, the excess of electrons in the well at this boundary caused by a large field gradient generates in region I a diffusion current opposite the current through the superlattice. Usually the diffusion backflow of electrons is compensated by a local increase of the field. This compensation is possible only if the current through the superlattice is smaller than the maximum current in region I.

The condition Eq. (18) also implies that there exists an upper limit of the field in the low-field region. When this field exceeds that limit value, the system becomes unstable. The development of the instability leads to the

expansion of the high-field region and the field in the low-field region reduces abruptly.

V. DESCRIPTION OF THE HIGH-FIELD REGION

In the high-field region the main contribution into the current is the electron tunneling from the first level of one well to the second level of the neighbor well followed by the relaxation from the second level to the first level. The main mechanism of the energy relaxation is the emission of optical phonons if the intersubband energy space $\mathcal{E}$ is larger than the phonon energy $\hbar\Omega_{\rm LO}$. In this case the relaxation time τ_{21} ranges from 0.5×10^{-12} to 10^{-11} sec depending on the intersubband energy space.[20,21,13,22–25] It is larger than the relaxation time in the bulk material because the scattering probability is inversely proportional to the transfer momentum squared and the transfer momentum in the intersubband relaxation $2m\sqrt{\mathcal{E}-\hbar\Omega_{\rm LO}}$ is larger than that in the bulk material $2m(\sqrt{E}-\sqrt{E-\hbar\Omega_{\rm LO}})\approx 2m\hbar\Omega_{\rm LO}/\sqrt{E}$; see Ref. 14. In the case of $\mathcal{E}<\hbar\Omega_{\rm LO}$ the main relaxation mechanism is the electron-electron interaction and τ_{21} is about $10^{-10}-10^{-9}$ sec.[26,13,15] The transition time τ_t can vary in a wide range depending on superlattice parameters. This time has been measured in 40 Å/40 Å and in 30 Å /30 Å GaAs–GaAlAs superlattices (see Ref. 27) and appeared at about 3.6×10^{-11} sec and 5.3×10^{-12} sec, respectively. In a 123 Å/21 Å superlattice τ_t has been found to be about 6×10^{-11} sec; see Ref. 25.

In the case when the first and the second level in adjacent wells are not in resonance one cannot use the simple balance equation Eq. (1). The current j_{12} in region II is described by Eq. (4b) with $i=1$ and $i'=2$. The energy space between these levels $\Delta=eF_\nu d-\mathcal{E}<0$. The current is equal to the number of electrons that relax from the second level to the first level per unit time

$$j_{12}=e\frac{n^{(2)}}{\tau_{21}}\ . \tag{20}$$

For simplicity we neglect in these calculations $\exp(-\mathcal{E}/T)$ compared to unit because usually $\mathcal{E}\gtrsim T$. So the generalized balance equations become

$$\frac{n(\zeta^{(1)}+\Delta)-n^{(2)}}{\tau_t}=\frac{n^{(2)}}{\tau_{21}}\ , \tag{21a}$$

$$n(\zeta^{(1)})+n^{(2)}=\bar{n}. \tag{21b}$$

In these equations the inverse transition time $1/\tau_t=2\Lambda_{12}^2\Gamma/\hbar(\Delta^2+\Gamma^2)$.

The eliminating of $n^{(2)}$ from Eqs. (21) leads to

$$j=\frac{e}{\hbar}\frac{2\Lambda_{12}^2\Gamma n(\zeta^{(1)}+\Delta)}{\Delta^2+\Gamma^2+2\Lambda_{12}^2\Gamma\tau_{21}/\hbar}\ . \tag{22}$$

This equation, together with Eq. (21), describes the current-voltage characteristics of the high-field domain, that is, the dependence of the current on the potential drop per period Fd. In general, this quantity is different from the value corresponding to the resonance between the first level in one well and the second level in the neighbor well $\mathcal{E}/e$. Usually it is assumed that the deviation from the resonance is negligibly small.[1,4,8] Actually the levels can be considered to be in resonance only if $|\Delta|\lesssim\Gamma$. However, it is not always true.

The results of Sec. IV show that the current in the superlattice with the high-field domain is smaller than j^*. If τ_{21} is not very large, then

$$j^*\ll e\bar{n}/2\tau_{21}\ . \tag{23}$$

In the other possible case $j^*\approx e\bar{n}/2\tau_{21}$, the levels have to be in the resonance and therefore $\Delta\approx0$. The condition Eq. (23) means that $n^{(2)}\ll\bar{n}$ and the last inequality is satisfied in two cases $n(\zeta^{(1)}-|\Delta|)\ll\bar{n}$ and $\tau_t\gg\tau_{21}$. In the first case

$$|\Delta|>T,E_F\ , \tag{24a}$$

i.e., the deviation from resonance is rather large. In the second case $\Delta^2+\Gamma^2\gg2\Lambda_{12}^2\Gamma\tau_{21}/\hbar$. Usually $\Gamma\sim3$–5 meV, $\tau_{21}>0.5\times10^{-12}$ sec, $\Lambda_{12}\gtrsim3$–5 meV, and therefore $\Gamma\lesssim\Lambda_{12}^2\tau_{21}/\hbar$, that is, in this case

$$|\Delta|\gg\sqrt{\Lambda_{12}^2\Gamma\tau_{21}/\hbar}\gtrsim\Gamma\ . \tag{24b}$$

These inequalities for Δ show that under the condition, Eq. (23), the increase of the applied bias, necessary for the extension of the high-field domain by one period, can be considerably smaller than the resonance value $\mathcal{E}/e$.

The limitation of the current by the value of j^* originates from the boundary between regions I and II; see Sec. IV. When with the increase of the bias the high-field domain extends over the entire superlattice, this boundary disappears. Then the current jumps up sharply and reaches the value defined by the conditions of the resonant tunneling

$$j_{\rm res}=\frac{\bar{n}}{\tau_t+2\tau_{21}}=\frac{e}{\hbar}\frac{2\Lambda_{12}^2\bar{n}}{\Gamma+4\Lambda_{12}^2\tau_{21}/\hbar}\ . \tag{25}$$

VI. LOW-FIELD REGION DOWNSTREAM OF THE DOMAIN

In this region, if it exists, electrons are injected into the second miniband from the high-field domain. They can move 1000 Å before they drop down to the first miniband.[14] The injection of electrons into the first miniband can be neglected. Therefore the current in the first miniband vanishes near the boundary with the high-field domain and increases away from it, owning to the relaxation from the second miniband.

In doped superlattices the screening length is about one period. In other words, the drop of the field at the boundary between regions II and III causes the depletion of only one well closest to the high-field domain and all other wells in region III can be considered to be electroneutral. The relaxation of electrons from the second miniband, where their mobility is high, into the first

miniband, where the electron mobility is much smaller, leads to field inhomogeneity on the scale of the relaxation length. We calculate the field distribution in the most interesting case, when this length is much larger than the superlattice period.

The relaxation length large compared to the superlattice period and to the screening length allows us to use the condition of electroneutrality and to replace difference equations with differential ones. The total current j is the sum of the currents in the first miniband j_1 and in the second miniband j_2

$$j = j_1 + j_2 \ , \tag{26a}$$

$$j_1 = \mu_1 \left(n^{(1)} eF - T \frac{dn^{(1)}}{dx} \right) \Big/ d \ , \tag{26b}$$

$$j_2 = \mu_2 \left(n^{(2)} eF - T \frac{dn^{(2)}}{dx} \right) \Big/ d \ , \tag{26c}$$

where μ_1 and μ_2 are the mobilities in the first and the second miniband, respectively. Here we assume the Boltzmann distribution in both minibands and neglect the field dependence of the mobilities. The first assumption is reasonable because one can expect a significant heating of electrons injected in region III. The second assumption is natural due to the following circumstance. The field dependence of the mobility is appreciable when the field is close enough to the instability threshold field $F_{\rm th}$. Usually the field in the high-field domain F_H is significantly larger than $F_{\rm th}$. Equation (19) shows that in this case j^* is significantly smaller than j_0 and therefore F_∞ cannot be close to $F_{\rm th}$. In the part of region III where the current moves mostly in the second miniband, the field is even smaller.

The conditions of the electroneutrality and the continuity equations are

$$n = n^{(1)} + n^{(2)}, \tag{26d}$$

$$\frac{dj_2}{dx} = -\frac{en^{(2)}}{\tau_{21} d} \ . \tag{26e}$$

In the general case the electric field can be found from Eqs. (26b)–(26d),

$$\frac{F}{F_\infty} = \frac{j_1}{j} + \frac{\mu_1}{\mu_2} \frac{j_2}{j} = 1 - \left[1 - \frac{\mu_1}{\mu_2} \right] \frac{j_2}{j} \ , \tag{27}$$

where F_∞ is the electric field far from the domain. After eliminating the current j_2 and the concentration $n^{(2)}$ from Eqs. (26c), (26e), and (27) one can get the differential equation for the field in region III

$$L_{\mathcal{D}}^2 \frac{d^2}{dx^2} \frac{F}{F_\infty} = L_{\rm dr} \frac{F}{F_\infty} \frac{d}{dx} \frac{F}{F_\infty} + \frac{F}{F_\infty} - 1 \ . \tag{28}$$

The redistributing of electrons between two minibands and the field profile are characterized by two lengths: a diffusion length $L_{\mathcal{D}}$ and a drift length $L_{\rm dr}$, where

$$L_{\mathcal{D}}^2 = \frac{\mu_2 \tau_{21} T}{e} \tag{29}$$

and

$$L_{\rm dr} = \mu_2 \tau_{21} F_\infty \ . \tag{30}$$

The former length is the distance that electrons diffuse in the second miniband before the relaxation to the first miniband. The latter length is the distance that electrons run in the second miniband under the electric field before the relaxation. Equation (28) will be solved near the boundary for an arbitrary relation between these two lengths. Far from the boundary we calculate the distribution of the electric field separately in two limit cases, when one of these two lengths is much larger than the other.

At $x = 0$ there is no current in the first miniband and Eq. (27) gives the boundary condition for Eq. (28),

$$\left. \frac{F}{F_\infty} \right|_{x=0} = \frac{\mu_1}{\mu_2} \ . \tag{31}$$

One can see that near the boundary, F/F_∞ is small if $\mu_1 \ll \mu_2$. That can be expected because the second miniband is usually wider than the first miniband. Thus we can neglect F/F_∞ with respect to the right-hand side of Eq. (28). This simplification allows us to solve this equation in terms of the Airy functions. The result is

$$\frac{F}{F_\infty} = -\left(4 \frac{L_{\mathcal{D}}^2}{L_{\rm dr}^2} \right)^{1/3} \frac{{\rm Ai}'((x - x_0)/L_0)}{{\rm Ai}((x - x_0)/L_0)} \ , \tag{32}$$

where ${\rm Ai}'(\xi)$ denotes the derivative of the Airy function with respect to its argument and $L_0 = (2L_{\mathcal{D}}^4/L_{\rm dr})^{1/3}$. The other parameter x_0 can be found by substitution of Eq. (32) into the boundary condition Eq. (31). This gives, for $\xi = -x_0/L_0$,

$$q = -{\rm Ai}'(\xi)/{\rm Ai}(\xi) \ , \tag{33}$$

where $q = (\mu_1/\mu_2)(L_{\rm dr}^2/4L_{\mathcal{D}}^2)^{1/3}$.

The solution Eq. (32) shows that the electric field increases away from the boundary. Far from the boundary where $F \sim F_\infty$, the solution Eq. (32) is not valid anymore. In the case of a short drift length $L_{\rm dr} \ll L_{\mathcal{D}}$ one can neglect the first term on the right-hand side of Eq. (28) because it contains a small parameter $L_{\rm dr}/L_{\mathcal{D}}$, which can be shown by the replacement of $x/L_{\mathcal{D}}$ with a dimensionless variable. In this case the solution to Eq. (28) is

$$\frac{F}{F_\infty} = \frac{j_1}{j} + \frac{\mu_1}{\mu_2} \frac{j_2}{j} = 1 - \left[1 - \frac{\mu_1}{\mu_2} \right] \exp(-x/L_{\mathcal{D}}) \ , \tag{34}$$

where the point $x = 0$ corresponds to the boundary between regions II and III. The characteristic length of the electron relaxation from the second miniband to the first one is in this case the diffusion length $L_{\mathcal{D}}$.

In the opposite case when $L_{\rm dr} \gg L_{\mathcal{D}}$, Eq. (28) can be simplified in the region where $(L_{\mathcal{D}}/L_{\rm dr})^{2/3} \ll F/F_\infty$, namely, the term on the left-hand side of Eq. (28) can be neglected. The solution to the resulting equation is

$$F/F_\infty - \ln(1 - F/F_\infty) = (x - x_0)/L_{\rm dr} \ . \tag{35}$$

Here x_0 is the same number as in Eq. (32). This can be proved by matching the asymptotics of both

solutions Eqs. (32) and (35) in the region where $(L_{\mathcal{D}}/L_{\rm dr})^{2/3} \ll F/F_\infty \ll 1$.

The very important property of Eqs. (26) is that the number of electrons in the second miniband explicitly depends on the interminiband relaxation time. One can get from Eq. (32) together with Eqs. (26e) and (27)

$$n^{(2)}|_{x=0} = 2\left[q^3 - q\xi(q)\right] n \,. \tag{36}$$

The parameter q, which defines the number of electrons in the second miniband near the boundary with region II, is proportional to $\tau_{21}^{1/3}$. When q is small $\xi \approx -1$ and $n^{(2)}(0) \approx 2qn$. When q is large the asymptotic of the Airy function gives $q \approx \xi^{-1}/4 + \xi^{1/2}$ and $n_2 \approx n$. The concentration $n^{(2)}$ as a function of q is plotted in Fig. 4.

The obtained field distribution is not valid at the distance about the screening length from the high-field domain because the electroneutrality condition Eq. (26d) cannot be used there. Thus in the well at the boundary between regions II and III (see Fig. 1), where the field changes significantly, the concentration of electrons has to be found from the Poisson equation. The field change near the next well $\nu = \nu_{\rm II} + 1$ is much smaller and we can consider it and the rest of region III as electroneutral. Therefore the solution to Eqs. (26) is valid up to the well number $\nu = \nu_{\rm II} + 1$ and $n^{(2)}_{\nu_{\rm II}+1} = n^{(2)}|_{x=0}$. The field in the barrier between well numbers $\nu_{\rm II}$ and $\nu_{\rm II} + 1$ can be easily computed from Eqs. (4a) and (8b) with $\nu = \nu_{\rm II}$. In the case when the relaxation length of the electrons from the second miniband to the first one is much larger than one superlattice period we can neglect the current between first levels and also put in Eq. (4a) $j_{11} = 0$ and $j_{22} = j$.

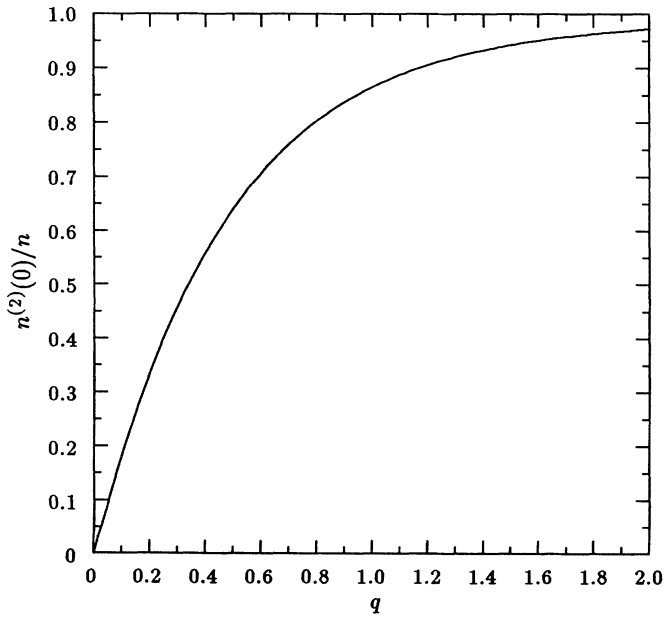

FIG. 4. The concentration of the electrons in the second miniband in region III of the superlattice close to the boundary with region II is plotted versus the parameter $q = (e\mu_1^3\tau_{21}F_\infty^2/\mu_2^2 T)^{1/3}$.

VII. DISCUSSION

In this section we give a qualitative description of the current-voltage characteristic of the entire superlattice. Under a small external bias the superlattice exhibits Ohm's law. At a higher bias the current reaches a maximum value. The uniform potential distribution in the superlattice is unstable at this point of the I-V characteristic. The theory of instability was developed by the present authors.[16,18] The instability eventually leads to the formation of the high-field domain and a sharp current drop. In Sec. II we argued that due to the charge accumulation at the high-field domain boundary, its length can be more than one superlattice period. Now we estimate this length.

The threshold value of the bias just before the instability point is $NF_{\rm th}d$, where N is the number of the superlattice periods. Right after the instability point this bias is a sum of the voltage drop across the high-field region $F_H N_{\rm II} d$ and the low-field region $\approx (N - N_{\rm II})F_\infty d$. Here we neglect the field inhomogeneity near the domain boundaries. So we have

$$NF_{\rm th}d = F_H N_{\rm II} d + (N - N_{\rm II})F_\infty d \tag{37}$$

and

$$N_{\rm II} = N\frac{F_{\rm th} - F_\infty}{F_H - F_\infty} \,. \tag{38}$$

This equation shows that in very long superlattices the length of the high-field domain is proportional to the length of the superlattice. This fact is a direct consequence of the upstream diffusion current near the boundary of the high-field domain. Without the diffusion the minimal length of the high-field domain is one superlattice period and $F_{\rm th} - F_\infty \propto 1/N$. Due to the diffusion current, F_∞ is limited from above by a value independent of the superlattice length. From Eqs. (9a), (18), and (19) we have

$$\sqrt{F_H^2 + 3F_{\rm th}^2} - F_H \geq F_\infty \,. \tag{39}$$

For $F_{\rm th} \geq F_\infty$ one can easy see that $N_{\rm II}$ decreases monotonically with increasing F_∞. Then Eqs. (38) and (39) give the following condition for $N_{\rm II}$:

$$N_{\rm II} \geq N\frac{F_H + 3F_{\rm th} - \sqrt{F_H^2 + 3F_{\rm th}^2}}{3(F_H + F_{\rm th})} \,. \tag{40}$$

Actually the field in regions I, II, and III is inhomogeneous. As a result there is a correction to the right-hand side of Eq. (40). Usually this correction can be neglected because it does not contain the factor N.

With a further increase of the bias the current nearly periodically increases and drops down. After Esaki and Chang,[1] each oscillation is associated with the extension of the high-field domain by one period and the number of oscillations $N_{\rm osc}$ is expected to be equal to $N - 1$. Equation (40) shows that $N_{\rm osc}$ can be less than $N - 1$ and that is really the case in some experiments. For instance, Kawamura *et al.*[2] observed a current-voltage character-

istic with $N_{osc} = 35$ in a superlattice that had $N = 39$ barriers. The difference between N and N_{osc} can be interpreted as the formation of a high-field domain with the minimal length $N_{II} = 4$. The value of the threshold field $F_{th}d$ in this experiment can be obtained by dividing the threshold voltage ≈ 0.5 V by the number of the superlattice barriers. The voltage drop across a barrier in the high-field domain $F_H d$ equals the period of the oscillations 0.14 V. The substitution of these values into Eq. (40) gives $N_{II} > 3.1$, which is in agreement with the value obtained from the number of the oscillations.

In order to understand how a large domain comes about, we performed a numerical calculation of the instability development. The simulation was made for a 30-period superlattice with the intersubband energy separation 100 meV and the electron concentration corresponding to the Fermi energy 40 meV. We assume some reasonable relations between transition and relaxation times. The parameters characterizing screening in the superlattice were $\lambda_1^2 = 4$ and $\lambda_2^2 = 8$. The results of the simulation are shown in Figs. 5 and 6. One can see that the domain starts to grow as a large scale instability[18] that transforms into a narrow domain with a length of three periods.

In the case of a low doping there are not enough electrons to form the depletion layer downstream of the domain. As a result the domain is formed near the anode[10] and region III does not exist. The position of the high-field domain in a highly doped superlattice is determined by unintentional nonuniformity of the superlattice or by a fluctuation that initiated the domain. For a field larger than F_{th}, the oscillating current is limited from above by the value of j^*. It is important to note that this value is usually smaller than j_0, i.e., the current value at $F = F_{th}$; see Sec. IV. Such a feature of the I-V characteristic is typically observed in experiment.[2,8]

We will show now that the high-field domain expands by joining another period from region I even in the case when region III does exist. For this purpose we make use of an equation similar to Eq. (37), where we take into account the nonuniformity of the field at the accumulation layer near the domain boundary. So instead of Eq. (37)

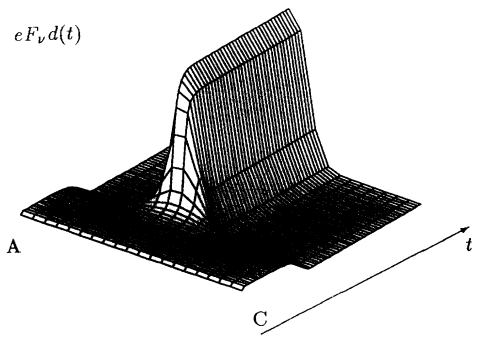

FIG. 5. The time evolution of the voltage drop distribution. The superlattice has 20 periods. The cathode and the anode are marked by C and A, respectively. The interlevel space in the well is 100 meV, whereas the domain height is only 70 meV per period.

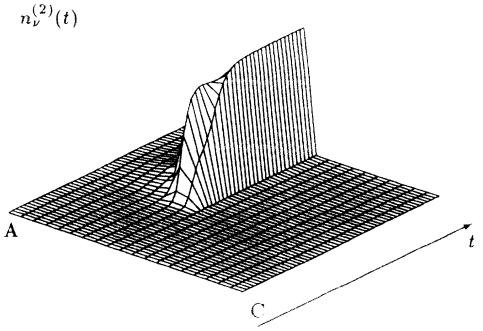

FIG. 6. The time evolution of the concentration at the second level in each well. The superlattice has 20 periods. The cathode and the anode are marked by C and A, respectively. One can see the tail of the electron distribution in region III (behind the domain).

we have

$$V = ed\sum_\nu F_\nu = [(N_I - 1)F_\infty + F_{\nu_I - 1} + N_{II}F_H]d + V_{III} , \quad (41)$$

where V is the applied bias, N_I and N_{II} are the numbers of periods in regions I and II, respectively, ν_I is the number of the first barrier in the high-field domain, and V_{III} is the potential drop across region III. Equation (41) resembles Eq. (37); however, it explicitly takes into account the field inhomogeneity in regions I and III.

As the applied voltage increases, dV/dj goes to the infinity which eventually leads to the current discontinuity and the extension of the high-field domain by one period. One can see from Eq. (41) that $dV/dj \to \infty$ when in one of the barriers $dF/dj \to \infty$. This cannot take place in region II, where the maximum value of the current is larger than that in region I. The infinite value of dF/dj or the zero value of dj/dF is ultimately connected with the maximum in the I-V characteristic of one barrier. This maximum is reached only in the regions where current is confined in the first miniband, i.e., in region I and in a part of region III. The largest field in these regions is in the last barrier of region I, $F_{\nu_I - 1}$; see the end of Sec. IV. The field in this barrier corresponding to $dF/dj \to \infty$ is larger than F_{th} for the following reason. In this barrier $dj/dF = dj_{cond}/dF + dj_{diff}/dF$. Since the field in region I grows faster than in region II, the concentration in the well between these regions decreases. Therefore the diffusion current also decreases, which means that $dj_{diff}/dF > 0$ because the diffusion current is directed against the conduction current. As a result $dj/dF = 0$ not when $dj_{cond}/dF = 0$ (i.e., $F = F_{th}$), but when $dj_{cond}/dF < 0$ (i.e., $F > F_{th}$).

The field in region II is about $\mathcal{E}/ed$ and the field in region I is smaller or about $F_{th} = \Gamma/ed$. Usually Γ is only a few meV. So, in experiments with a big energy separation,[2,3] $\mathcal{E} \approx 200$ meV, the field difference between regions I and II is also large and it causes a large charge accumulation at the boundary between these regions. In these experiments $eF_H d \approx 140$ meV, $eF_{th}d \approx 12.5$ meV,

and so $F_{th}/F_H \approx 0.089$ and Eq. (19) gives $j^* \approx 0.30 j_0$. That value is in good agreement with the ratio of the maximum of the current in the oscillating region to the peak value of the current at the instability threshold; see Fig. 2(b) in Ref. 2.

The oscillations of the current in a superlattice with a high-field domain caused by the expansion of this domain with an increase of the applied bias have a period which can be associated with the potential drop per the superlattice period in the high-field region $F_H d$. However, Eq. (24) shows that the potential drop per period in the domain is less than the energy separation between levels $\mathcal{E}$ by a significant quantity, which can reach a few tens of meV.

Such a big difference between the period of the oscillations of the current-voltage characteristic and the energy separation between the levels was detected in the experiment of Kawamura *et al.*;[3] see Fig. 3 in the cited work. One can see that the difference between the intersubband energy space and the electric current oscillation period increases with $\mathcal{E}$. This has a simple physical meaning: in samples with larger $\mathcal{E}$, the upper limit of the current j^* is lower and therefore the resonance in region II is weaker. Other examples on such a difference can be found in Refs. 4, 6 and 28.

The main assumption made in our calculation concerns a small deviation of the electron distribution function from the Fermi function with effective temperature and chemical potential. Necessary conditions justifying this assumption (see Sec. III) may not be satisfied in the high-field domain. However, the features of the current-voltage characteristic discussed in present work do not depend on the detailed shape of the electron distribution.

In conclusion, we have studied the field distribution and I-V characteristic of the superlattice in the voltage region when a high-field domain exists. The accumulation of electrons at the domain boundary causes a strong limitation of the current. Due to this limitation the minimal length of the high-field domain can be not one, but a few superlattice periods. The current limitation also results in a reduction of the period of the current oscillations compared to that corresponding to the energy separation between the first and the second level in a well. These results are in good agreement with available experimental data. The field distribution in the region downstream of the high-field domain (if it exists) is nonuniform due to electron relaxation from the second miniband to the first miniband.

[1] L. Esaki and L. L. Chang, Phys. Rev. Lett. **33**, 495 (1974).
[2] Y. Kawamura, K. Wakita, H. Asahi, and K. Kurumada, Jpn. J. Appl. Phys. **25**, L928 (1986).
[3] Y. Kawamura, K. Wakita, and K. Oe, Jpn. J. Appl. Phys. **26**, L1603 (1987).
[4] K. K. Choi, B. F. Levine, R. J. Malik, J. Walker, and C. J. Bethea, Phys. Rev. B **35**, 4172 (1987).
[5] B. F. Levine, K. K. Choi, C. J. Bethea, J. Walker, and R. J. Malik, Appl. Phys. Lett. **50**, 1092 (1987).
[6] K. K. Choi, B. F. Levine, C. J. Bethea, J. Walker, and R. J. Malik, Appl. Phys. Lett. **50**, 1814 (1987).
[7] K. K. Choi, B. F. Levine, N. Jarosik, J. Walker, and R. J. Malik, Phys. Rev. B **38**, 123 62 (1988).
[8] T. H. H. Vuong, D. C. Tsui, and W. T. Tsang, J. Appl. Phys. **66**, 3688 (1989).
[9] M. Helm, P. England, E. Colas, F. DeRosa, and S. J. Allen, Phys. Rev. Lett. **63**, 74 (1989).
[10] H. T. Grahn, H. Schneider, and K. von Klitzing, Phys. Rev. B **41**, 2890 (1990).
[11] A. Sibille, J. F. Palmier, and F. Mollot, Appl. Phys. Lett. **60**, 457 (1992).
[12] S. H. Kwok, T. B. Norris, L. L. Bonilla, J. Galán, F. C. Martínez, J. M. Molera, H. T. Grahn, K. Ploog, and R. Merlin (unpublished).
[13] M. Artaki and K. Hess, Phys. Rev. B **37**, 2933 (1988).
[14] D. C. Herbert, Semicond. Sci. Technol. **3**, 101 (1988).
[15] V. I. Falko, Phys. Rev. B **47**, 13 585 (1993).
[16] B. Laikhtman, Phys. Rev. B **44**, 11 260 (1991).
[17] F. Prengel, A. Wacker, and E. Schöll, Phys. Rev. B **50**, 1705 (1994).
[18] B. Laikhtman and D. Miller, Phys. Rev. B **48**, 5395 (1993).
[19] R. F. Kazarinov and R. A. Suris, Fiz. Tekn. Poluprovodn. **6**, 120 (1972) [Sov. Phys. Semicond. **6**, 120 (1972)].
[20] C. H. Yang and S. A. Lyon, Physica **134B**, 305 (1985).
[21] A. Seilmeier, H.-J. Hübner, G. Abstreiter, G. Weimann, and W. Schlapp, Phys. Rev. Lett. **59**, 1345 (1987).
[22] J. K. Jain and S. Das Sarma, Phys. Rev. Lett. **62**, 2305 (1989).
[23] R. J. Bäuerle, T. Elaesser, W. Kaiser, H. Lobentanzer, W. Stolz, and K. Ploog, Phys. Rev. B **38**, 4307 (1988).
[24] M. C. Tatham, J. F. Ryan, and C. T. Foxon, Phys. Rev. Lett. **63**, 1637 (1989).
[25] H. T. Grahn, H. Schneider, W. W. Rühle, K. von Klitzing, and K. Ploog, Phys. Rev. Lett. **64**, 2426 (1990).
[26] D. Y. Oberli, D. R. Wake, M. V. Klein, J. Klem, T. Henderson, and H. Morkoç, Phys. Rev. Lett. **59**, 696 (1987).
[27] B. Deveaud, A. Chomette, B. Lambert, and A. Regreny, Solid State Commun. **57**, 885 (1986).
[28] H. T. Grahn, Phys. Scr. **T49**, 507 (1993).